Prepared for the
NATIONAL AERONAUTICS AND SPACE ADMINISTRATION

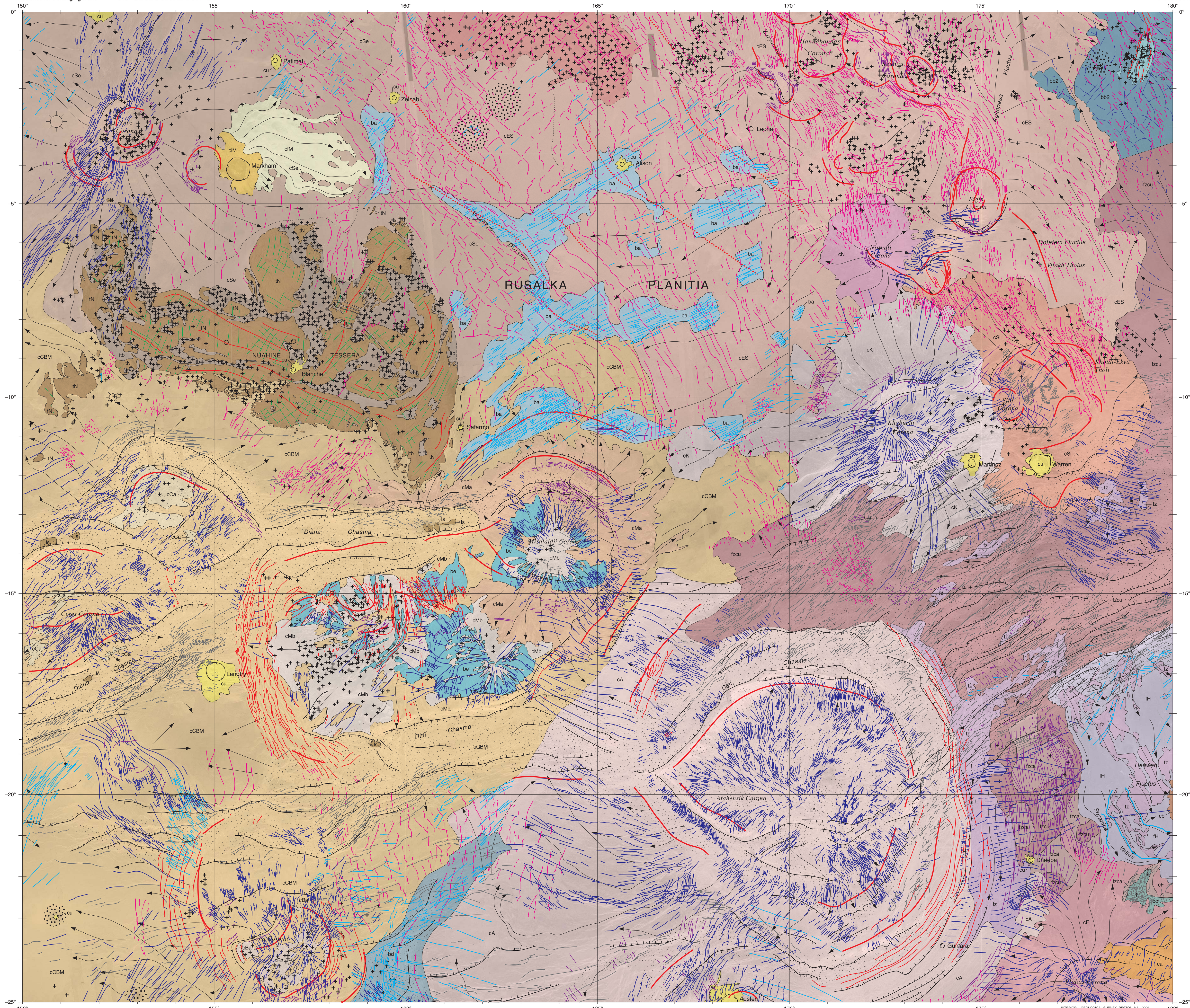

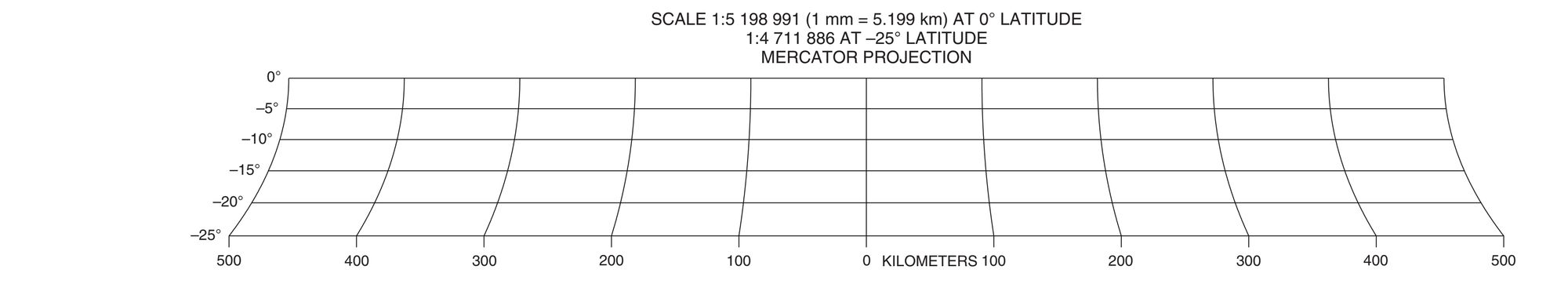

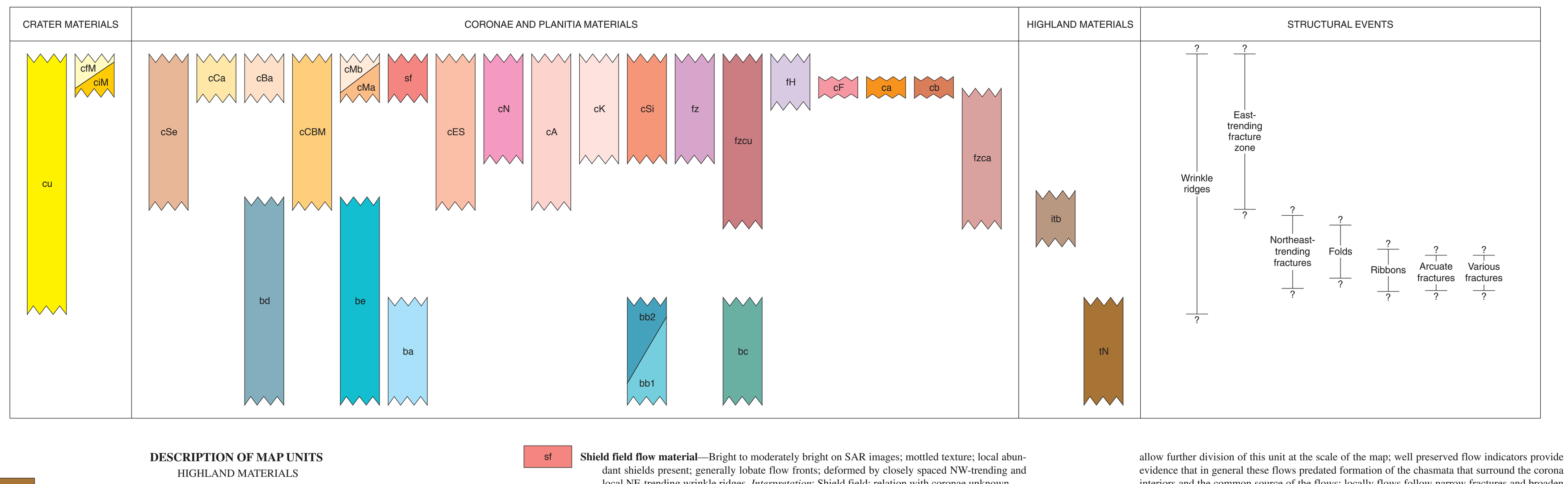

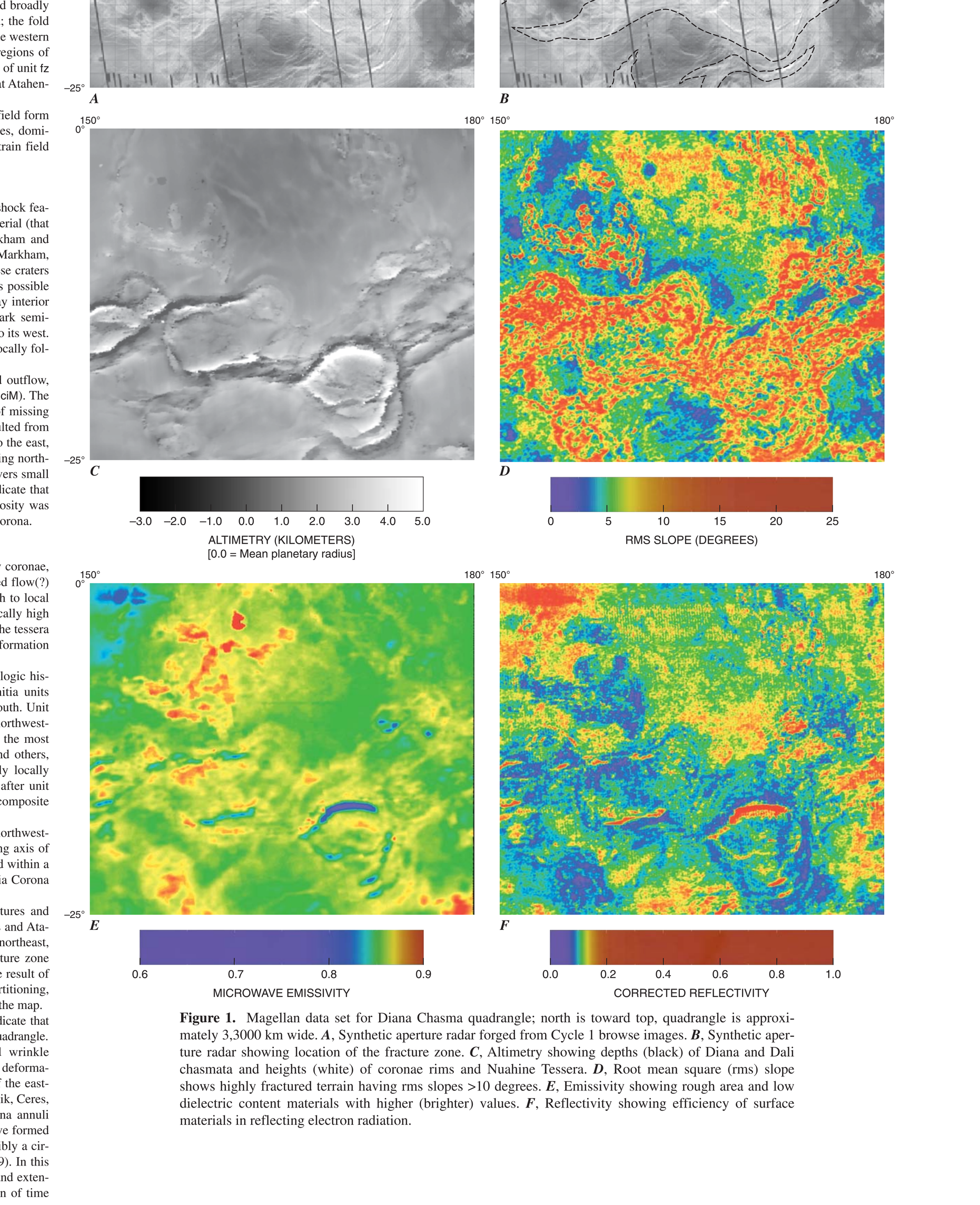

Figure 1. Magellan data set for Diana Chasma quadrangle; north is toward top, quadrangle is approximately 3,3000 km wide. ***A***, Synthetic aperture radar forged from Cycle 1 browse images. ***B***, Synthetic aperture radar showing location of the fracture zone. ***C***, Altimetry showing depths (black) of Diana and Dali chasmata and heights (white) of coronae rims and Nuahine Tessera. ***D***, Root mean square (rms) slope shows highly fractured terrain having rms slopes >10 degrees. ***E***, Emissivity showing rough area and low dielectric content materials with higher (brighter) values. ***F***, Reflectivity showing efficiency of surface materials in reflecting electron radiation.

Table 1. *Crater data for Diana Chasma quadrangle.*

Name	Latitude (° S.)	Longitude (° E.)	Diameter (km)	Unit location	Ejecta blanket	Impact halo	Central peak	Rim	Interior flooding	Deformation and notes
Alison	4.0	165.6	14.4	ba	Y	N	Y	Y	Y	None—partial interior flooding only; timing relations to wrinkle ridges unknown
Austen	25.0	168.4	45.1	cA	Y	N	Y	Y	N	Yes—ejecta covers Atahensik fractures but cut by fractures related to corona south of map area
Blanche	9.3	157.0	12.3	itb	Y	Y	N	Y	N	None—ejecta flows follow tessera structures and flow north, following current topography
Dheepa	21.6	176.3	4.7	fzcu	Y	Y	N	Y	N	None—ejecta flows follow preexisting fractures
Gulnara	23.7	174.0	5.0	cA	Y	N	N	N	N	Yes—highly degraded; post-dates fold formation
Langtry	17.0	155.0	50.3	cCBM	Y	N	N	Y2	Y	Yes—flooded interior heavily fractured; ejecta cut by fracture zone fractures
Leona	3.1	169.0	3.0	cES	Y	N	N	Y	N	None—ejecta deposited in broadly radial ray pattern; timing relations to wrinkle ridges unknown
Markham	4.1	155.6	71.8	cSe	Y	N	Y	Y	Y	None—extensive lava flows follow current topography, flow toward basin to the east; flows buttressed by wrinkle ridges and locally follow preexisting fractures
Martinez	11.7	174.7	23.5	cK	Y	N	Y	Y	Y	Yes—ejecta covers some fractures but not others; dark interior of crater cut by fractures; heavily deformed region makes delineation of discrete fracture set difficult
Patimat	1.3	156.5	5.1	cSe	Y	Y	Y	Y	N	None—diffuse wind-blown material thins to west; ejecta covers wrinkle ridges
Safarmo	10.8	161.4	7.4	cCBM	Y	N	Y	Y	N	Yes—ejecta locally cut by regionally late-forming NNE-trending fractures
Warren	11.7	176.5	50.9	cSi	Y	N	Y	Y	Y	Yes—heavily degraded and deformed ejecta blanket; interior flooding by two materials (radar bright and radar dark) exhibits small amounts of deformation
Zeinab	2.2	159.6	12.5	cES	Y	N	Y	Y	Y	None—flooded interior undeformed; timing relations to wrinkle ridges unknown
a	8.6	157.1	3.0	tN	P	N	N	P	--	Possible small crater
b	8.6	155.3	3.0	tN	P	N	N	P	--	Possible small crater
c	22.9	150.9	2.5	cCBM	Y	Y	N	Y	N	None—diffuse halo blankets surrounding structures
d	9.3	152.8	12.9	tN	N	N	N	P	Y	Possible small crater
	2.3	162.5	--	cES	N	N	N	N	N	Shock feature
	3.1	161.7	--	cES	N	N	N	N	N	Shock feature
	1.4	178.2	--	bb2	N	N	N	N	N	Shock feature
	24.9	153.0	--	cCBM	N	N	N	N	N	Shock feature

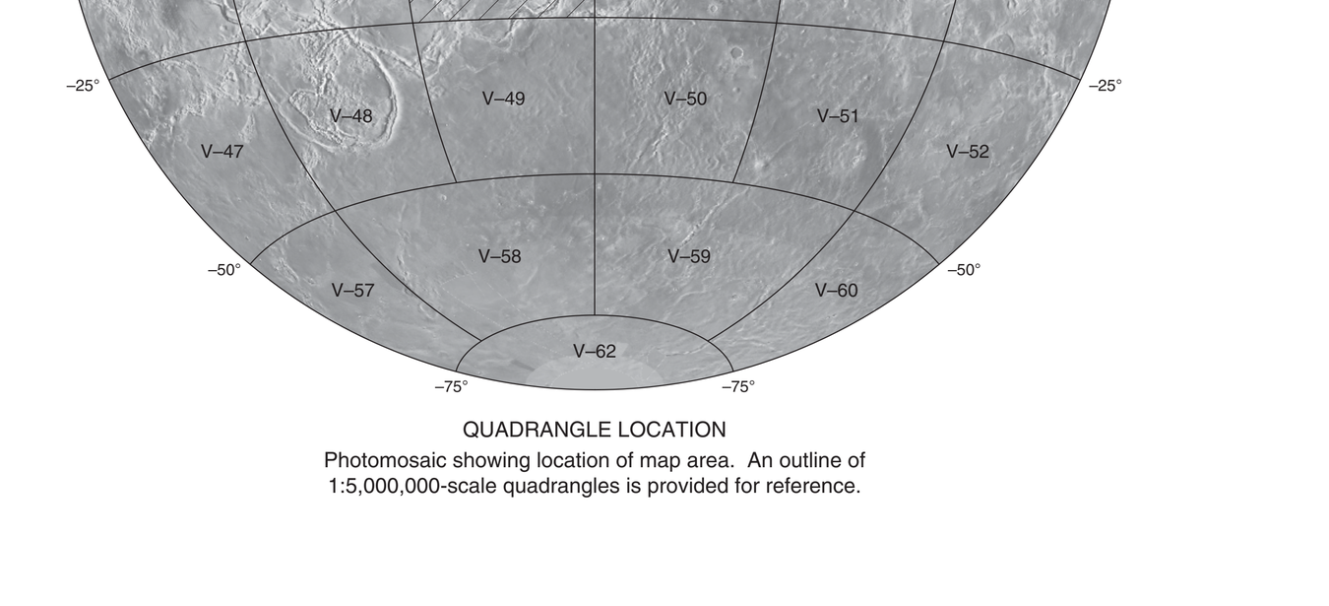

QUADRANGLE LOCATION
Photomosaic showing location of map area. An outline of 1:5,000,000-scale quadrangles is provided for reference.

This unit may extend to the contact with units tN and itb as shown on the map, or the unit could end north of this boundary as indicated by the dotted contact (see map), in which case an additional basal unit must be considered. As discussed above, an additional basal unit might exist—such a unit would likely predate units cSe and cES, yet it must postdate the emplacement and deformation of unit ba. Given the absence of solid evidence for such a unit, we have chosen the simplest geologic relations that are consistent with the available data and extended units cSe and cES to the east and west, respectively, to their lowest topographic points and interpreted a contact relation between them. We also chose to extend unit cSe to the contact with units tN and itb in the south. Unit cSe is a composite unit of diachronous flows as indicated by detailed flow and fracture relations. Earlier flows are cut by north-northeast-trending Seia-related fractures, yet other flows cover these same fractures.

These coronae-related fold belts differ from the fold belt preserved in the northeast corner of the map area in their association with coronae. The northeast fold belt hosts north-trending folds that were clearly active over an extended timeframe relative to surface flows and resulted in exposure of unit bb1. Detailed geologic relations indicate intimate relations between flow formation and uplift, similar to the detailed history documented for ridge belts in the Baltis Vallis region of V–13 quadrangle (Stewart and Head, 2000). Various levels of terraces are preserved along the fold belt margins, and the folds variably deform flows. This fold belt, which also is host to numerous shields, parallels a more

Izenberg, N.R., Arvidson, R.E., and Phillips, R.J., 1994, Impact crater degradation on venusian plains: Geophysical Research Letters, v. 21, p. 289–292.
Kaula, W.M., 1990, Venus: A contrast in evolution to Earth: Science, v. 247, p. 1191–1196.
Keep, M., and Hansen, V.L., 1994, Structural evolution of Maxwell Montes, Venus: Implications for venusian mountain "belt" formation: Journal of Geophysical Research, v. 99, p. 26,015–26,028.
Kirk, R.L., Soderblom, L.A., and Lee, E.M., 1992, Enhanced visualization for interpretation of Magellan radar data—Supplement to the Magellan special issue: Journal of Geophysical Research, v. 97, no. E10, p. 16,371–16,380.
Kryuchkov, V.P., 1988, Ridge belts on the plains of Venus, in Abstracts submitted to the Nineteenth Lunar and Planetary Science Conference, March14–18, 1988: Houston, Lunar and Planetary Institute, p. 649–650.
McKenzie, D., Ford, P.G., Johnson, C., Parsons, B., Sandwell, D.T., Saunders, S., and Solomon, S.C., 1992, Features on Venus generated by plate boundary processes: Journal of Geophysical Research, v. 97, no. E8, p. 13,533–13,544.
Pavri, B., Head, J.W., Klose, K.B., and Wilson, L., 1992, Steep-sided domes on Venus: Characteristics, geologic setting, and eruption conditions from Magellan data: Journal of Geophysical Research, v. 97, no. E8, p. 13,445–13,478.
Phillips, R.J., and Hansen, V.L., 1998, Geological evolution of Venus: Rises, plains, plumes and plateaus: Science, v. 279, p. 1492–1497.
Plaut, J.J., 1993, Stereo imaging, *in* Ford, J.P., Plaut, J.J., Weitz, C.M., Farr, T.G., Senske, D.A., Michaels, G., Parker, T.J., Guide to Magellan image interpretation: Jet Propulsion Laboratory Publication 93–24, p. 33–41.

GEOLOGIC MAP OF THE DIANA CHASMA QUADRANGLE (V–37), VENUS

By
Vicki L. Hansen and Heather R. DeShon

2002

For sale by U.S. Geological Survey, Information Services, Box 25286, Federal Center, Denver, CO 80225, 1–888–ASK–USGS

ISBN 0-607-98067-2

Printed on recycled paper